Cadherin-11 in Synovial Lining Formation and Pathology in Arthritis

David M. Lee, *et al.*

Science **315**, 1006 (2007);
DOI: 10.1126/science.1137306

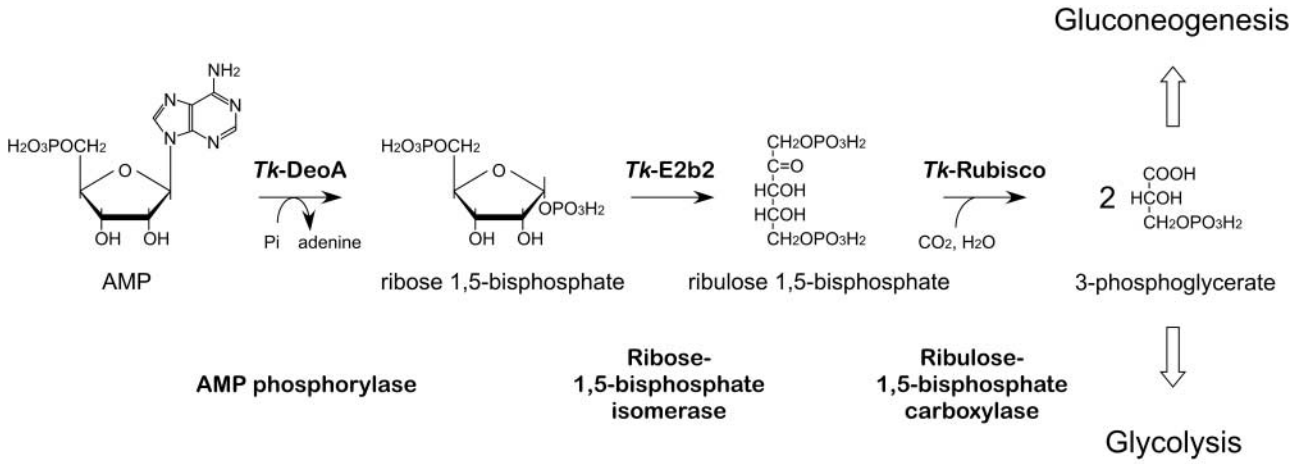

Fig. 2. A metabolic pathway composed of homologs of DeoA, aIF2B, and type III RuBisCOs.

conversion of 3-PGA to fructose 6-phosphate (gluconeogenesis). If the non-oxidative branch of the pentose phosphate pathway were to be responsible for pentose synthesis, the cyclic pathway would constitute a CO_2 fixation pathway (fig. S4). Although their genome sequences are not available, there are several autotrophic strains in the Crenarchaeota that exhibit RuBisCO activity despite lacking phosphoribulokinase activity (*25*).

Type III RuBisCOs seem to have a function distinct from that of the classical RuBisCOs in the CBB pathway of *Bacteria* and *Eucarya*. When considering that the organisms harboring type III RuBisCOs represent relatively deep and short lineages in evolution, it may well be that the carboxylase activity of RuBisCO originally evolved to function in this pathway.

References and Notes

1. R. J. Ellis, *Trends Biochem. Sci.* **4**, 241 (1979).
2. G. M. F. Watson, F. R. Tabita, *FEMS Microbiol. Lett.* **146**, 13 (1997).
3. J. M. Shively, G. van Keulen, W. G. Meijer, *Annu. Rev. Microbiol.* **52**, 191 (1998).
4. S. Ezaki, N. Maeda, T. Kishimoto, H. Atomi, T. Imanaka, *J. Biol. Chem.* **274**, 5078 (1999).
5. G. M. F. Watson, J.-P. Yu, F. R. Tabita, *J. Bacteriol.* **181**, 1569 (1999).
6. T. E. Hanson, F. R. Tabita, *Proc. Natl. Acad. Sci. U.S.A.* **98**, 4397 (2001).
7. H. Ashida *et al.*, *Science* **302**, 286 (2003).
8. N. Maeda *et al.*, *J. Mol. Biol.* **293**, 57 (1999).
9. K. Kitano *et al.*, *Structure* **9**, 473 (2001).
10. N. Maeda, T. Kanai, H. Atomi, T. Imanaka, *J. Biol. Chem.* **277**, 31656 (2002).
11. M. W. Finn, F. R. Tabita, *J. Bacteriol.* **185**, 3049 (2003).
12. J. W. Wray, R. H. Abeles, *J. Biol. Chem.* **270**, 3147 (1995).
13. A. Sekowska, A. Danchin, *BMC Microbiol.* **2**, 8 (2002).
14. A. Sekowska *et al.*, *BMC Microbiol.* **4**, 9 (2004).
15. T. Fukui *et al.*, *Genome Res.* **15**, 352 (2005).
16. Materials and methods are available as supporting material on *Science* Online.
17. F. Gebauer, M. W. Hentze, *Nat. Rev. Mol. Cell Biol.* **5**, 827 (2004).
18. L. D. Kapp, J. R. Lorsch, *Annu. Rev. Biochem.* **73**, 657 (2004).
19. C. G. Proud, *Semin. Cell Dev. Biol.* **16**, 3 (2005).
20. M. W. Finn, F. R. Tabita, *J. Bacteriol.* **186**, 6360 (2004).
21. M. R. Walter *et al.*, *J. Biol. Chem.* **265**, 14016 (1990).
22. S. W. M. Kengen, J. E. Tuininga, F. A. M. de Bok, A. J. M. Stams, W. M. de Vos, *J. Biol. Chem.* **270**, 30453 (1995).
23. B. Siebers, P. Schönheit, *Curr. Opin. Microbiol.* **8**, 695 (2005).
24. A. Schiffer, G. Fritz, P. M. H. Kroneck, U. Ermler, *Biochemistry* **45**, 2960 (2006).
25. M. Hügler, H. Huber, K. O. Stetter, G. Fuchs, *Arch. Microbiol.* **179**, 160 (2003).
26. S. Guindon, O. Gascuel, *Syst. Biol.* **52**, 696 (2003).
27. S. Guindon, F. Lethiec, P. Duroux, O. Gascuel, *Nucleic Acids Res.* **33**, W557 (2005).
28. This study was supported by a grant-in-aid for scientific research (no. 14103011 to T.I.), a grant-in-aid for scientific research on priority areas "Applied Genomics" (no. 18018026 to H.A.), and a grant for the Japan Society for the Promotion of Science fellows (no. 15005649 to T.S.) from the Ministry of Education, Culture, Sports, Science and Technology of Japan.

Supporting Online Material

www.sciencemag.org/cgi/content/full/315/5814/1003/DC1
Materials and Methods
Figs. S1 to S4
References

6 October 2006; accepted 8 January 2007
10.1126/science.1135999

Cadherin-11 in Synovial Lining Formation and Pathology in Arthritis

David M. Lee,[1] Hans P. Kiener,[1] Sandeep K. Agarwal,[1]* Erika H. Noss,[1]* Gerald F. M. Watts,[1]* Osamu Chisaka,[2] Masatoshi Takeichi,[3] Michael B. Brenner[1]†

The normal synovium forms a membrane at the edges of joints and provides lubrication and nutrients for the cartilage. In rheumatoid arthritis, the synovium is the site of inflammation, and it participates in an organized tissue response that damages cartilage and bone. We identified cadherin-11 as essential for the development of the synovium. Cadherin-11–deficient mice have a hypoplastic synovial lining, display a disorganized synovial reaction to inflammation, and are resistant to inflammatory arthritis. Cadherin-11 therapeutics prevent and reduce arthritis in mouse models. Thus, synovial cadherin-11 determines the behavior of synovial cells in their proinflammatory and destructive tissue response in inflammatory arthritis.

Cadherin adhesion molecules are a family of integral membrane proteins that contain five immunoglobulin (Ig)–like extracellular (cadherin) domains rigidified as an extended chain by interdomain calcium binding [reviewed in (*1*, *2*)]. Cadherins mediate cellular adhesion by binding a cadherin of the same type on an adjacent cell via interactions of the extracellular N-terminal first cadherin domains. During embryonic development, cadherins provide the basis for cell sorting, aggregation, and tissue morphogenesis (*1*–*3*). Postnatally, cadherins provide cell-to-cell adhesion within tissues, contributing to the maintenance of tissue integrity and architecture (*3*, *4*). Knowing these activities of cadherin proteins, we hypothesized that a mesenchymal cadherin may function to provide cell adhesion to organize the synovial membrane.

[1]Department of Medicine and Division of Rheumatology, Immunology and Allergy, Brigham and Women's Hospital, Harvard Medical School, 1 Jimmy Fund Way, Boston, MA 02115, USA. [2]Department of Cell and Developmental Biology, Graduate School of Biostudies, Kyoto University, Sakyo-ku, Yoshida-honmachi, Kyoto 606-8501, Japan. [3]RIKEN Center for Developmental Biology, Minatojima-Minamimachi, Chuo-ku, Kobe 650-0047, Japan.

*These authors contributed equally to this work.
†To whom correspondence should be addressed. E-mail: mbrenner@rics.bwh.harvard.edu

The synovium consists of a lining layer containing fibroblasts and macrophages that overlies a sublining layer of loose connective tissue. Using immunohistochemical staining, we found that the condensed lining layer of synoviocytes in healthy mice expresses cadherin-11 (Fig. 1, A and B). In a strain of mice that develops spontaneous autoimmune arthritis (K/BxN) (*5*, *6*), marked cadherin-11 expression was seen on cells with fibroblast morphology in the synovial lining and in the synovial pannus, a pathological outgrowth of synovial tissue derived from fibroblast-like synoviocytes (FLS) (Fig. 1, C and D). Particularly intense staining of cadherin-11 was also noted in FLS within the pannus adjacent to bone and cartilage.

To define which synovial cellular lineages express cadherin-11, we used multicolor cytofluorometric staining of freshly disaggregated joint tissues, using a newly generated monoclonal antibody (mAb) to cadherin-11 (anti-cadherin–11) (fig. S1) and CD45 (anti-CD45) (a marker of bone marrow–derived cells). Consistent with its expression on the FLS lineage in humans (*7*), we observed that cadherin-11 identifies a synovial population distinct from that identified by CD45 (Fig. 1, E and F). These findings were confirmed biochemically by fluorescence-activated cell sorting (FACS) isolation of CD45 or cadherin-11–expressing subpopulations. Western blotting of these sorted cells demonstrated no detectable cadherin-11 expression on the $CD45^+$ subpopulation (Fig. 1G). Previous studies have demonstrated that fibroblasts lining the synovium express CD55 (*8*). In our analyses, CD55 expression was seen on about half of cadherin-11^+ cells in arthritic joints (fig. S2). Cadherin-11 expression on cultured FLS, with the use of cell surface biotinylation and immunoprecipitaton with anti-cadherin–11, revealed the anticipated protein species of molecular weight 110,000 from wild-type FLS but not from FLS derived from cadherin-11–deficient mice (Fig. 1, H to J) (*9*). In addition, because cadherins associate with cytoplasmic β-catenin, we performed multicolor immunofluorescence microscopy and found colocalization of cadherin-11 with β-catenin in adherens junctions, specifically at sites of cell-to-cell contact between FLS (Fig. 1, K to M). By means of a cell-to-substrate adhesion assay (*10*), the ability of FLS derived from either wild-type or cadherin-11–deficient mice was assessed for binding to recombinant cadherin-11–Fc. Wild-type FLS demonstrated robust adhesion to cadherin-11–Fc, whereas cadherin-11–deficient FLS failed to adhere (Fig. 1N and fig. S1). These studies demonstrate cadherin-11 expression in murine synovial fibroblasts, the localization of cadherin-11 to adherens junctions, and the role of cadherin-11 in homophilic adhesion by synovial fibroblasts.

The functional contribution of cadherin-11 to synovial fibroblast organization in synovial tissues was next explored. When compared to wild-type synovium, cadherin-11–deficient synovium

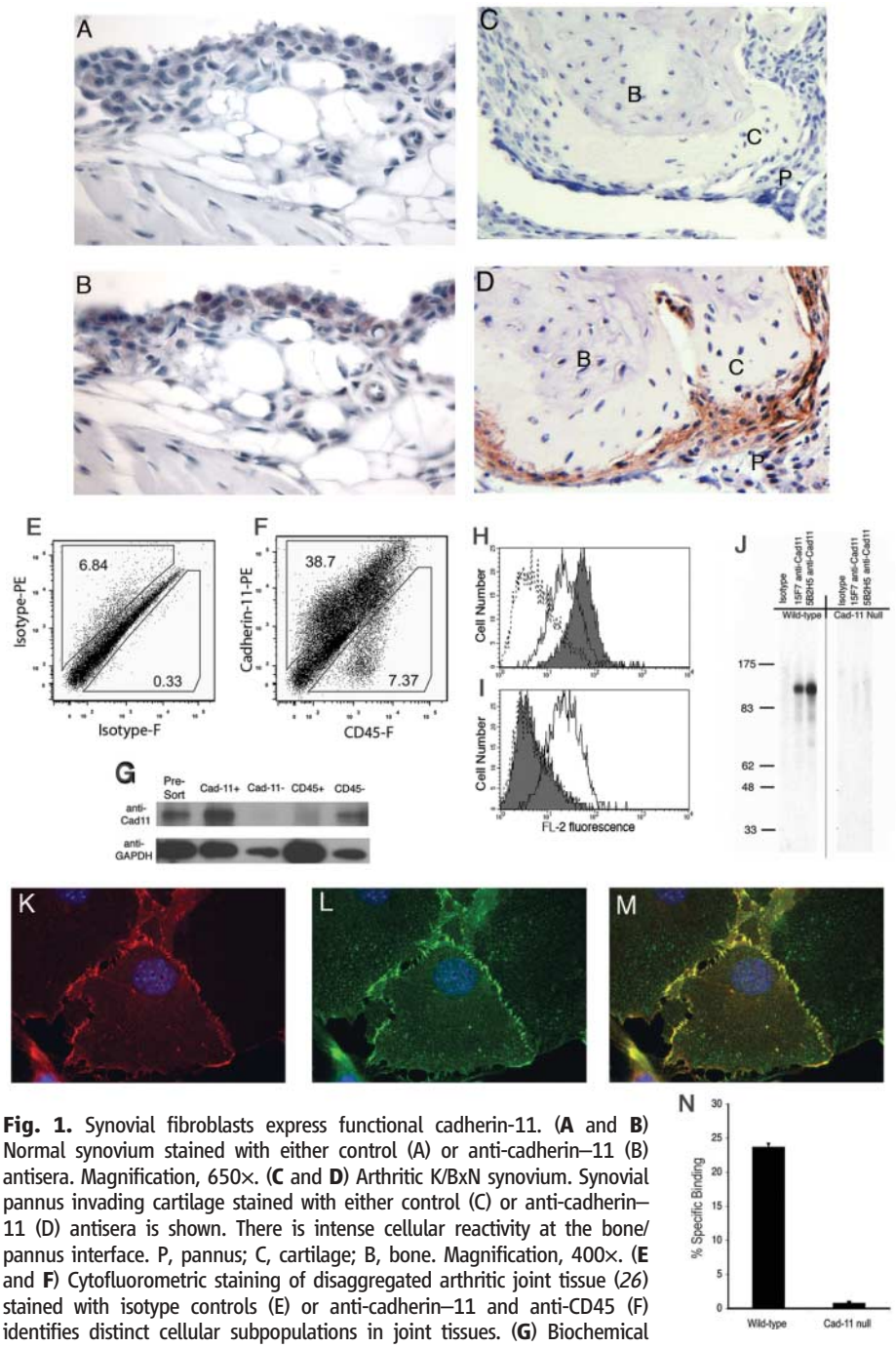

Fig. 1. Synovial fibroblasts express functional cadherin-11. (**A** and **B**) Normal synovium stained with either control (A) or anti-cadherin–11 (B) antisera. Magnification, 650×. (**C** and **D**) Arthritic K/BxN synovium. Synovial pannus invading cartilage stained with either control (C) or anti-cadherin–11 (D) antisera is shown. There is intense cellular reactivity at the bone/pannus interface. P, pannus; C, cartilage; B, bone. Magnification, 400×. (**E** and **F**) Cytofluorometric staining of disaggregated arthritic joint tissue (*26*) stained with isotype controls (E) or anti-cadherin–11 and anti-CD45 (F) identifies distinct cellular subpopulations in joint tissues. (**G**) Biochemical analysis of FACS-sorted synovial subpopulations. Dispersed arthritic joint tissues were labeled with either anti-CD45 or anti-cadherin–11 and sorted by means of FACS. Lysates of these subpopulations and presorted cells were analyzed by Western blot for cadherin-11 and glyceraldehyde-3-phosphate dehydrogenase (GAPDH) expression. There is an absence of detectable cadherin-11 expression in CD45-expressing cells. (**H** and **I**) Cytofluorometric staining of cultured FLS. FLS derived from wild-type (WT) (H) and cadherin-11–null (I) mice and passaged five times were stained with an anti-cadherin–11 mAb (gray fill), isotype control (dashed line), and an antibody to major histocompatibility complex class I (solid line). (**J**) Immunoprecipitation of cadherin-11 from cultured FLS. WT and cadherin-11–null FLS were surface biotinylated, lysed, and immunoprecipitated with isotype control Ig (IgG1) or anti-cadherin–11 (15F7 and 5B2H5). (**K** to **M**) FLS express cadherin-11 in adherens junctions. WT FLS were fixed and stained with anti-cadherin–11 (K) and anti–β-catenin (L) (*11*). The colocalization of cadherin-11 and β-catenin [(M), merged image] at sites of cellular interface is in a pattern consistent with that of adherens junctions. Magnification, 1000×. (**N**) Cadherin-11 mediates homophilic adhesion in FLS. WT and cadherin-11–null FLS were allowed to adhere to substrate cadherin-11–Fc in a cell-to-substrate adhesion assay (*10*). The homophilic adhesion of WT FLS to cadherin-11–Fc is absent in cadherin-11–null FLS. Error bars indicate SEM.

demonstrated marked hypoplasia of the synovial lining, with decreased synovial lining compaction and reduced membrane folds (Fig. 2, A to C). A primary function of FLS is the elaboration of extracellular matrix (ECM). Using Masson's trichrome stain to highlight ECM, we found that the dense ECM of the synovial lining, apparent in wild-type mice, was markedly attenuated in cadherin-11–null mice (Fig. 2, D and E). Thus, we conclude that cadherin-11 is necessary for cellular organization, compaction, and matrix elaboration of the synovial lining in vivo.

To further confirm the role of cadherin-11 in synovial tissue organization, we used a three-dimensional (3D) synovial micromass organ culture system in vitro (fig. S3A) (*11*). Single cell suspensions of wild-type and cadherin-11–null FLS were dispersed in a surrogate ECM, and synoviocyte capacity for lining layer formation was assessed. Wild-type FLS establish a condensed lining-like structure at the matrix/media interface with marked similarity to that seen in the synovial lining at the synovial fluid interface in vivo (Fig. 2F). In contrast, cadherin-11–null FLS micromass cultures failed to develop lining condensation or compaction (Fig. 2G). Thus, this in vitro model of synovial tissue function confirms that lining layer compaction is an inherent feature of synovial fibroblast behavior that relies on cadherin-11.

We next examined the role of cadherin-11 in synovial fibroblast behavior in the K/BxN serum transfer model of autoimmune inflammatory arthritis. In this model, passive transfer of arthritogenic autoantibodies elicits a distal symmetric erosive polyarthritis with pathology mediated by immune complex formation, complement activation, myeloid lineage cell activation, and elaboration of cytokines interleukin-1 and tumor necrosis factor (TNF) (*5*, *6*, *12*–*15*). Administration of arthritogenic K/BxN serum revealed a measurable resistance to clinical arthritis in cadherin-11–null mice (Fig. 3, A and B). Indeed, pooled data for the clinical index from these mice demonstrated an average 50% reduction of clinical arthritic activity in cadherin-11–null mice. This reduction suggests that cadherin-11 expressed on fibroblasts can substantially influence the severity of pathology in arthritis.

As in rheumatoid arthritis, murine models of inflammatory arthritis display hyperplasia and outgrowth of synovial tissue composed of synovial fibroblasts (pannus tissue). The pannus attaches to and migrates over bone and cartilage surfaces, locally invading and destroying these structures (*16*). Examination of inflamed joint tissue architecture from wild-type and cadherin-11–null mice demonstrated that the typical condensed hyperplastic synovial lining architecture in inflammatory arthritis is largely absent in cadherin-11–deficient mice (Fig. 3, C and D). Rather, the synovial architecture in cadherin-11–deficient mice was chaotic and loosely organized.

The 3D micromass organ culture provides a means of analyzing selected factors that modulate synovial fibroblast function in a simplified model of the complex synovial microenvironment. Wild-type and cadherin-11–null synovial micromass organ cultures were stimulated with TNF, a potent inflammatory cytokine implicated in rheumatoid arthritis. In contrast to the dramatic ultrastructural changes in wild-type cultures, which are characterized by surface lining cellular accumulation and condensation, only modest changes were apparent in cadherin-11–deficient synovial micromass organ cultures (Fig. 3, E and F).

The results thus far suggested that cadherin-11 might be a potentially useful therapeutic target. To examine this, we used a cadherin-11–Fc fusion protein and an anti-cadherin–11 mAb. Similar to the cadherin-11–null phenotype, administration of either reagent ameliorated K/BxN serum transfer arthritis activity in wild-type mice (Fig. 3, G and H). To examine a role for cadherin-11 in ongoing inflammatory arthritis, we assessed its ability to reduce established disease. Because the K/BxN serum transfer model of arthritis is rapid and self-limited, we used a variation of this model, administering arthritogenic serum weekly to drive persistent synovitis (Fig. 3I). After allowing at least 2 weeks of active arthritis, we administered anti-cadherin–11 or isotype control treatments for a period of 10 days and examined arthritis clinical responses (Fig. 3, I and J). Similar to our observations in preventing acute arthritis, we find that anti-cadherin–11 displays moderate amelioration of established arthritis. These observations provide evidence that cadherin-11 contributes to the regulation of arthritic tissue responses in both acute and chronic synovitis.

The ability of FLS to migrate and invade through ECM is a potentially important feature of tissue remodeling that forms the hyperplastic lining and accomplishes erosion into cartilage. Cadherins and especially mesenchymal cadherins, like cadherin-11, are known to influence cell migration and invasion (*17*). To gain further insight into the cadherin-11 regulation of FLS function, we performed migration and invasion assays through ECM-coated transwells. Although cadherin-11–null FLS display similar basal migratory activity to that of wild-type cells, their inducible migratory capacity was attenuated (Fig. 4A). Examination of platelet-derived growth factor (PDGF)–stimulated ECM invasive capacity revealed a dramatic deficit in cadherin-11–null FLS, which displayed only ~25% of the invasive activity of wild-type cells (Fig. 4B). These observations prompted us to examine cartilage and bone erosion in the inflammatory arthritis model in vivo. Indeed, synovial tissue attachment to, migration over, and

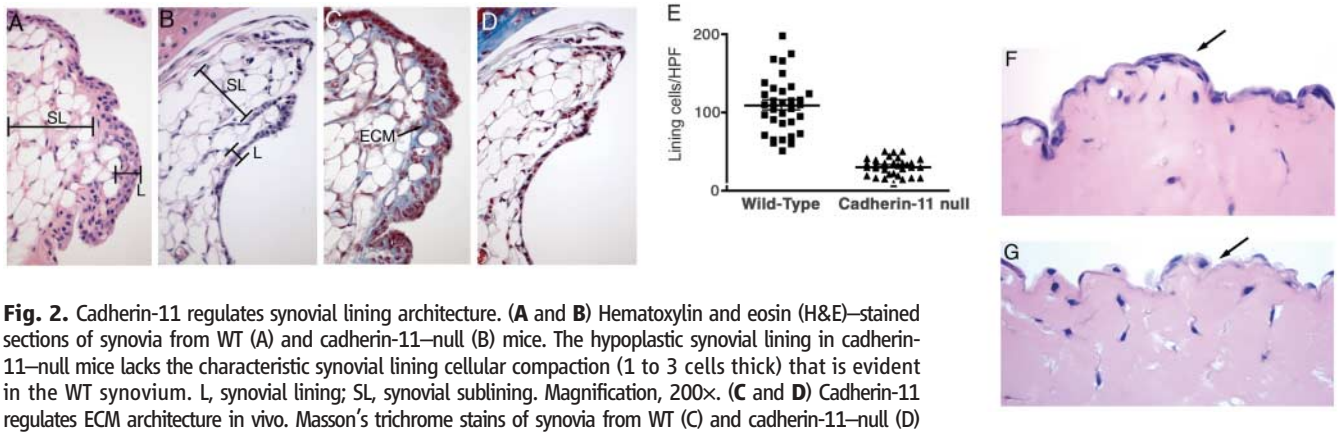

Fig. 2. Cadherin-11 regulates synovial lining architecture. (**A** and **B**) Hematoxylin and eosin (H&E)–stained sections of synovia from WT (A) and cadherin-11–null (B) mice. The hypoplastic synovial lining in cadherin-11–null mice lacks the characteristic synovial lining cellular compaction (1 to 3 cells thick) that is evident in the WT synovium. L, synovial lining; SL, synovial sublining. Magnification, 200×. (**C** and **D**) Cadherin-11 regulates ECM architecture in vivo. Masson's trichrome stains of synovia from WT (C) and cadherin-11–null (D) mice are shown. The hypoplastic synovial cellular lining (red) and markedly attenuated condensed ECM (blue) in cadherin-11–null mice as compared to those of the WT synovium are shown. Magnification, 200×. (**E**) Synovial lining cell density. Lining layer cells per high power field (HPF) (100 μM^2) were enumerated in WT (squares) and cadherin-11–null (triangles) mice. Individual results, mean, and SEM are provided. $n = 11$ mice per group; $P < 0.0001$. (**F** and **G**) Micromass organ culture lining compaction. WT (F) and cadherin-11–null (G) FLS were placed in micromass organ culture for 21 days (*11*) and were fixed, sectioned, and stained with H&E. The cellular condensation and lining formation behavior evident in WT FLS [arrow in (F)] and markedly attenuated in cadherin-11–null FLS [arrow in (G)] are shown. Magnification, 400×. Data are representative of five independent experiments.

invasion into cartilage were markedly diminished in cadherin-11–deficient mice. Wild-type synovial pannus caused full-thickness cartilage erosion, whereas cadherin-11–null synovial pannus stopped at the cartilage edge (Fig. 4, C and D, black arrowheads). Quantification by histomorphometric methods confirmed an 80% reduction in cartilage erosion in cadherin-11–deficient mice. By comparison, bone erosions, which are primarily dependent on osteoclast function (*18*–*20*), were evident to a similar degree in both wild-type and cadherin-11–null mice (Fig. 4E).

These studies suggest that, in healthy mice, cadherin-11 directs the establishment and maintenance of the normal synovial lining by conferring on FLS an ability to form cell-to-cell adhesion and compaction, as well as a capacity to produce ECM (Fig. 2). In the context of inflammatory arthritis, in which the synovium undergoes organized pathologic changes, mesenchymal lineage FLS contribute to these dramatic changes in the synovial lining (*21*–*24*). In cadherin-11–deficient mice, the synovial lining and synovial pannus tissue appeared architecturally aberrant and chaotic (Fig. 3, C and D), underscoring the role of cadherin-11 in fibroblast participation in the organized pathological synovial lining hyperplasia and pannus tissue destruction of cartilage in inflammatory arthritis.

The data suggest that cadherin-11 influences both the degree of inflammation (Fig. 3, A and B and G and H) and the organized pathologic response of the synovial tissue in response to arthritogenic K/BxN serum transfer (Fig. 4, C and E). In rheumatoid arthritis, the FLS population demonstrates a metabolically active, secretory state (*25*). Stimulation of FLS can induce secretion of a number of proinflammatory mediators that have been postulated to amplify and perpetuate synovial inflammation. Our findings suggest that cadherin-11 influences FLS participation in the synovial inflammatory reaction, in addition to its role in tissue remodeling and cartilage invasion. These insights identify previously unappreciated mechanisms governing the behavior of the joint lining and reveal the central role of a synovial cadherin in determining the behavior of the resident synovial mesenchy-

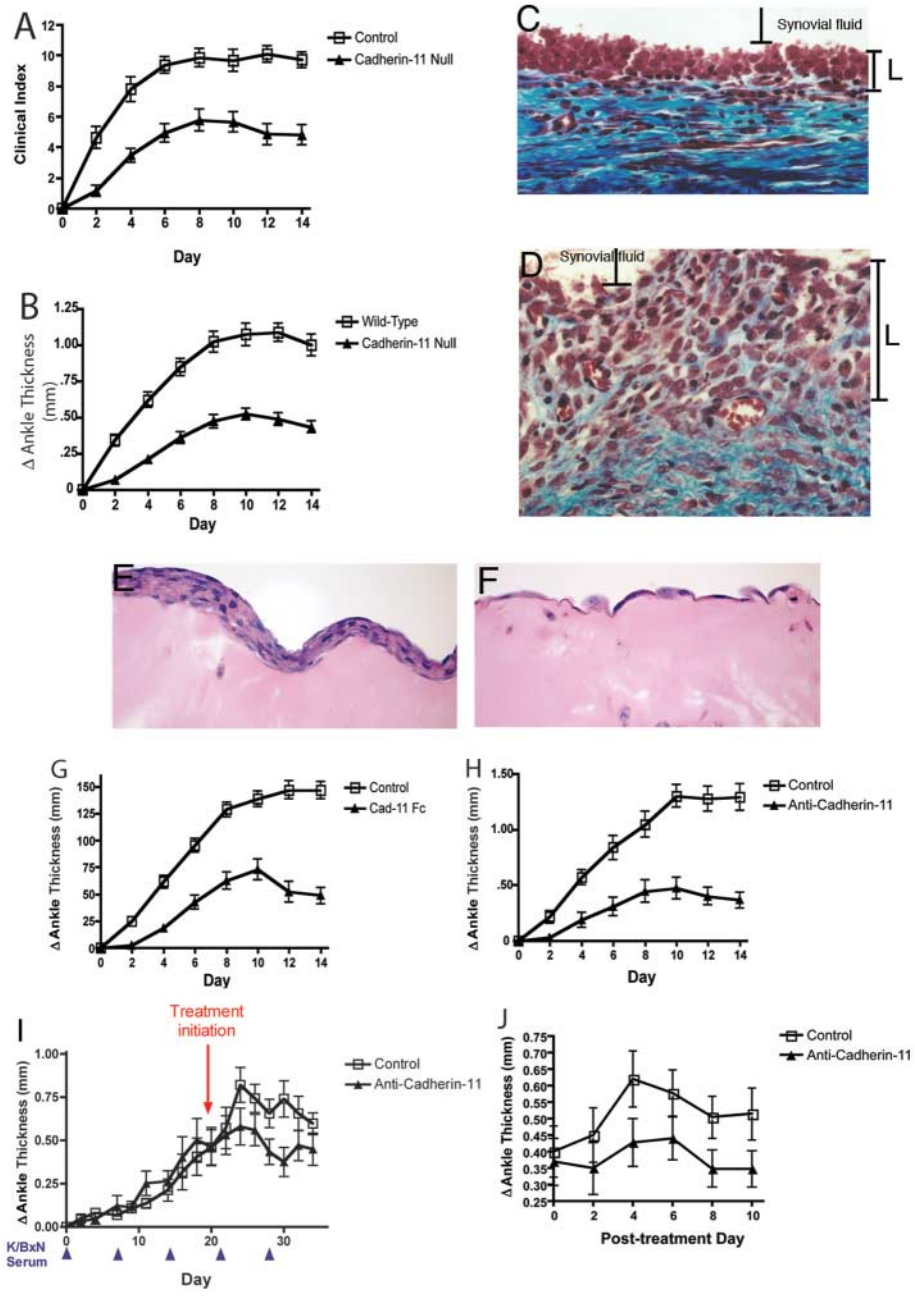

Fig. 3. Cadherin-11 modulates synovial tissue response in arthritis. (**A** and **B**) Cadherin-11–null mice are resistant to inflammatory arthritis. WT and cadherin-11–null mice were injected with arthritogenic K/BxN serum, and clinical index (A) and changes (Δ) in ankle thickness (B) were recorded over 2 weeks (*6*). Pooled results from 24 (WT) or 26 (cadherin-11–null) mice from four independent experiments ($P < 0.0005$) are shown. (**C** and **D**) Synovial architecture in inflammatory arthritis. Masson's trichrome–stained ankle sections from arthritic WT (C) and cadherin-11–null (D) mice demonstrate synovial lining hyperplasia (red) and dense ECM deposition (blue) in WT mice. In contrast, cadherin-11–null inflamed tissues demonstrate chaotic cellular organization within a minimal ECM. Synovial effusion in joint space is labeled. Magnification, 400×. (**E** and **F**) FLS lining architecture in vitro. WT (E) or cadherin-11–null (F) FLS micromass organ cultures (*11*) were exposed to TNF (10 ng/ml) for 21 days. The high degree of lining condensation and lining layer formation evident in WT FLS (E) is markedly aberrant in cadherin-11–null FLS (F). Magnification, 400×. Data are representative of three independent experiments. (**G** to **J**) Cadherin-11 biotherapeutics ameliorate inflammatory arthritis. WT C57BL/6 mice were injected with arthritogenic K/BxN serum [blue triangles in (I)] and co-injected [(G) and (H)] with control Ig (open squares) and with either cadherin-11–Fc [(G), solid triangles] or anti-cadherin–11 [(H), solid triangles] administered with a loading dose (0.5 mg) followed by maintenance dosing (0.1 mg) every 48 hours. Pooled results from 18 (cadherin-11–Fc) and 10 (anti-cadherin–11) mice are shown from four and two independent experiments, respectively. $P < 0.003$. For treatment studies [(I) and (J)], control Ig (open squares) or anti-cadherin–11 [(H), solid triangles] were administered for 10 days after allowing at least 2 weeks of arthritic activity. Results representative of two independent experiments (I) ($n = 5$ mice per group) and pooled treatment results (J) ($n = 10$ mice per group; $P = 0.0027$) are shown. Error bars in (A), (B), and [(G) to (J)] indicate SEM.

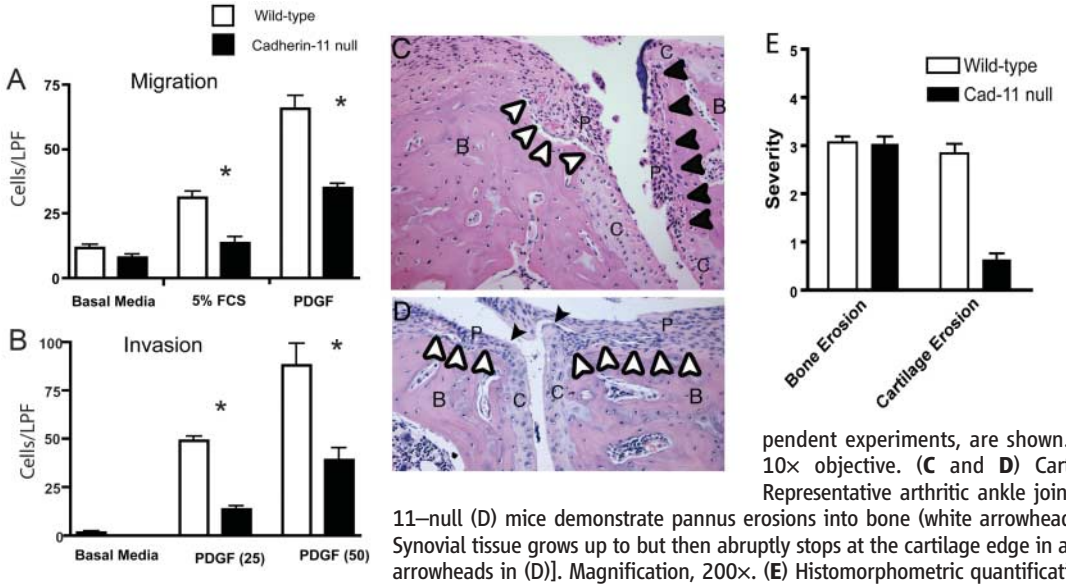

Fig. 4. Cadherin-11 regulates FLS invasive activity and cartilage erosion. (**A** and **B**) FLS migratory and invasive activity. FLS migratory activity was assessed in fibronectin-coated 8 μM transwell chambers (*17*) in the presence of basal media or stimulatory fetal calf serum (FCS) (5%) or PDGF. Invasive activity of WT (white bars) or cadherin-11–null (black bars) FLS was quantified in Matrigel ECM-coated transwells (*17*) in either basal media or PDGF (25 or 50 ng/ml). Mean ± SEM of quadruplicate counts from triplicate wells, representative of two independent experiments, are shown. *, $P < 0.01$. LPF, low power field, 10× objective. (**C** and **D**) Cartilage and bone erosions in vivo. Representative arthritic ankle joint tissues from WT (C) and cadherin-11–null (D) mice demonstrate pannus erosions into bone (white arrowheads) and cartilage (black arrowheads). Synovial tissue grows up to but then abruptly stops at the cartilage edge in arthritic cadherin-11–null mice [black arrowheads in (D)]. Magnification, 200×. (**E**) Histomorphometric quantification of bone and cartilage erosions in ankle tissues from WT and cadherin-11–null mice (*27*). There is a decrease in cartilage erosions in cadherin-11–null mice. Results are pooled data from 24 (WT) and 26 (cadherin-11–null) mice from four independent experiments. $P < 0.0001$. Error bars represent SEM.

mal cells in the dynamic and orchestrated tissue response in inflammatory arthritis.

References and Notes

1. B. M. Gumbiner, *Cell* **84**, 345 (1996).
2. M. Takeichi, *Curr. Opin. Cell Biol.* **7**, 619 (1995).
3. M. L. Hermiston, J. I. Gordon, *J. Cell Biol.* **129**, 489 (1995).
4. M. J. Wheelock, K. R. Johnson, *Annu. Rev. Cell Dev. Biol.* **19**, 207 (2003).
5. V. Kouskoff *et al.*, *Cell* **87**, 811 (1996).
6. D. M. Lee *et al.*, *Science* **297**, 1689 (2002).
7. X. Valencia *et al.*, *J. Exp. Med.* **200**, 1673 (2004).
8. M. E. Medof, E. I. Walter, J. L. Rutgers, D. M. Knowles, V. Nussenzweig, *J. Exp. Med.* **165**, 848 (1987).
9. K. Horikawa, G. Radice, M. Takeichi, O. Chisaka, *Dev. Biol.* **215**, 182 (1999).
10. J. M. Higgins *et al.*, *J. Cell Biol.* **140**, 197 (1998).
11. H. P. Kiener, D. M. Lee, S. K. Agarwal, M. B. Brenner, *Am. J. Pathol.* **168**, 1486 (2006).
12. I. Matsumoto *et al.*, *Nat. Immunol.* **3**, 360 (2002).
13. I. Matsumoto, A. Staub, C. Benoist, D. Mathis, *Science* **286**, 1732 (1999).
14. H. Ji *et al.*, *Immunity* **16**, 157 (2002).
15. H. Ji *et al.*, *J. Exp. Med.* **196**, 77 (2002).
16. D. M. Lee, H. P. Kiener, M. B. Brenner, in *Kelley's Textbook of Rheumatology*, E. D. Harris Jr. *et al.*, Eds. (Saunders, St. Louis, ed. 7, 2004).
17. M. T. Nieman, R. S. Prudoff, K. R. Johnson, M. J. Wheelock, *J. Cell Biol.* **147**, 631 (1999).
18. K. Redlich *et al.*, *J. Clin. Invest.* **110**, 1419 (2002).
19. A. R. Pettit *et al.*, *Am. J. Pathol.* **159**, 1689 (2001).
20. Y. Y. Kong *et al.*, *Nature* **402**, 304 (1999).
21. H. R. Schumacher, R. C. Kitridou, *Arthritis Rheum.* **15**, 465 (1972).
22. J. P. Kulka, D. Bocking, M. W. Ropes, W. Bauer, *Arch. Pathol.* **59**, 129 (1955).
23. B. Henderson, E. R. Pettipher, *Semin. Arthritis Rheum.* **15**, 1 (1985).
24. N. A. Athanasou, J. Quinn, *Ann. Rheum. Dis.* **50**, 311 (1991).
25. C. Hollywell, C. J. Morris, M. Farr, K. W. Walton, *Virchows Arch. A Pathol. Anat. Histopathol.* **400**, 345 (1983).
26. Materials and methods are available as supporting material on *Science* Online.
27. M. Chen *et al.*, *J. Exp. Med.* **203**, 837 (2006).

28. This work was funded by NIH grants K08 AR2214 (D.M.L.) and R01 AR48114 (M.B.B.), the Cogan Family Foundation (D.M.L.), the Arthritis Foundation Investigator Award (D.M.L.) and Fellowship Award (H.P.K. and E.H.N.), the Riva Foundation (M.B.B.), and an Abbott Scholar Award in Rheumatology Research (S.K.A.). M.B.B. and D.M.L. have equity holdings in Synovex Incorporated, which develops therapeutics for rheumatoid arthritis, and D.M.L. is a paid consultant to Resolvyx, Repligen, MedImmune, UCB Pharma, and MEDAcorp. The authors acknowledge the expert histotechnical assistance of T. Bowman.

Supporting Online Material

www.sciencemag.org/cgi/content/full/1137306/DC1
Materials and Methods
Figs. S1 to S3

8 November 2006; accepted 22 December 2006
Published online 25 January 2007;
10.1126/science.1137306
Include this information when citing this paper.